Smart Simplification of Anthropomorphic Head Phantom Aimed for Microwave Imaging

Tushar Singh, S Abedi, B Ninkovic, M Stevanovic, N. Joachimowicz, Hélène Roussel, B Kolundzija

Smart Simplification of Anthropomorphic Head Phantom Aimed for Microwave Imaging

T. Singh[1,2], S. Abedi[3], B. Ninkovic[2], M. Stevanovic[1], N. Joachimowicz[3], H. Roussel[3], B Kolundzija[1,2]

[1] School of Electrical Engineering, University of Belgrade, Belgrade, Serbia, mnikolic@etf.rs

[2] WIPL-D, Belgrade, Serbia, tushar.singh@wipl-d.com

[3] Sorbonne Université, CNRS, Laboratoire de Génie Electrique et Electronique de Paris, 75252 - Paris, France.
Université Paris-Saclay, CentraleSupélec, CNRS, Laboratoire de Génie Electrique et Electronique de Paris,
91192 - Gif-sur-Yvette, France. soroush.abedi@sorbonne-universite.fr

Abstract—**In this paper we study the numerical modeling of the complex anthropomorphic human phantoms, aimed for microwave imaging, using the WIPL-D software. By comparing various models, we investigate the influence of the geometrical simplification of the phantom on the accuracy of the electromagnetic response of the antennas in the vicinity of the phantom. By controlling the geometrical deviation of the simplified model with respect to the original model, we show that it is possible to reduce the simulation resources for one to two orders of magnitude while preserving the precision of the electromagnetic analysis.**

Index Terms—**microwave imaging, numerical modeling, anthropomorphic phantoms.**

I. INTRODUCTION

Medical microwave imaging (MWI) is one of the fastest progressing areas due to the utilization of non-ionizing radiation and affordable components [1], [2]. Currently, the golden standards in medical diagnostics are magnetic resonance imaging (MRI) and X-ray computerized tomography (CT), which provide high-resolution images. However, such systems are expensive and non-portable, which are significant drawbacks in many applications, such as patient bedside monitoring. Among many potential MWI applications, microwave brain imaging has gained a particular interest [3]-[5]. The justification for utilizing MWI in brain diagnostics lies in a considerable permittivity contrast between the healthy and stroke tissues in the microwave region [1]. However, several limitations prevent wide-spread utilization of MWI systems. One is their relatively low resolution compared to that of MRI and CT scans, and the other is the high computational cost of microwave imaging algorithms.

In this paper, we focus on increasing the speed of electromagnetic simulation of an anthropomorphic phantom by reducing the geometrical complexity of the model, while preserving the accuracy of the calculations. This is in contrast to our previous work [6], in which we studied the possibility to reduce the level of inhomogeneity of human tissue models by applying the mixing formulas. For numerical computation, we use the full-wave EM solver WIPL-D [7]. As an initial model, we use the human head phantom obtained from the MRI scans [8], [9].

In this study, we define two quality measures – the first one determines the geometrical deviation of the simplified model from the original and the second one is the relative error for the transmission between a pair of dipoles due to the reduction of the model.

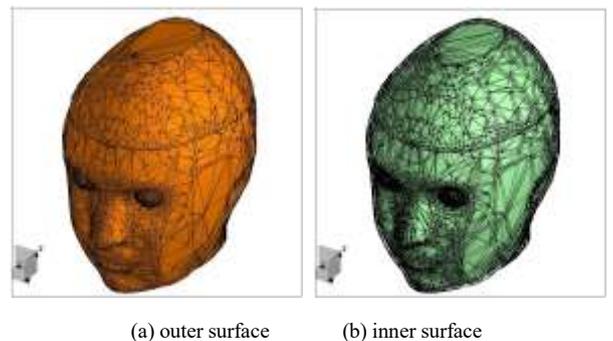(a) outer surface   (b) inner surface

Fig. 1.   The numerical phantom is represented by a triangular mesh.

The paper is organized as follows. After the Introduction, in Section II we describe the anthropomorphic head phantom. In Section III we define the quality measures and study the performance of the models with different levels of complexity. Finally, in the conclusion, we discuss the obtained results and give guidelines for future work.

II. ANTHROPOMORFIC PHANTOM

For the purpose of analysis, we used the anthropomorphic human phantom, which was obtained by modifying the original data from the Athinoula A. Martinos Center for Biomedical Imaging at Massachusetts General Hospital [8]. The phantom description was given in the stereo-lithography (STL) format and Fig. 1 shows the associated triangular mesh. The corresponding physical phantom is made of polyester casting resin and has already been used for testing and validation of a microwave imaging system [10].

The phantom is approximately 26 cm high and 3 mm thick. The largest cross section has an elliptical shape, with the minor and major axes being equal to 20 cm and 26 cm, respectively. The electromagnetic parameters of the numerical phantom are the same as those of the physical phantom at 1 GHz, described in [10]. The permittivity and conductivity of the material used for phantom printing is Acrylonitrile Butadiene Styrene (ABS) of relative permittivity and conductivity, $\varepsilon_r = 3$ and $\sigma = 0.004\,\mathrm{S/m}$ respectively. The

interior of the phantom is filled with a homogeneous substance whose dielectric constant and conductivity correspond to the weithted values of the permittivity and conductivity of the white (75%) and gray matter (25%) ($\varepsilon_r = 42$ and $\sigma = 1\,\mathrm{S/m}$). Such properties can be achieved using a liquid mixture, made of Triton X-100, water and salt [10]. Inside the homogeneous brain there is a stroke, modeled as a sphere with a three centimeters diameter. For the electromagnetic properties of the stroke, we used the corresponding data for the blood, i.e., $\varepsilon_r = 61$ and $\sigma = 1.8\,\mathrm{S/m}$ at 1 GHz. The phantom is immersed in a matching medium, whose parameters are $\varepsilon_r = 18.425$ and $\sigma = 0.2\,\mathrm{S/m}$.

III. NUMERICAL MODEL

The phantom was originally defined using the very fine triangular mesh. As shown in Fig. 1, the number of triangles is extremely dense around eyes, ears and lips - i.e., head parts that are not essential in stroke detection.

From the perspective of numerical efficiency, it is more favorable to use a) a quadrilateral mesh instead of a triangular one, and b) higher order bases instead of lower order bases [11]. Conversion from triangles to quadrilaterals can be done in a brute force manner in which every triangle is converted into the three quadrilaterals. However, to reduce the number of unknowns, neighboring triangles are first merged into quadrilaterals if the angle between their surface normals is less than five degrees. Such small angle tolerance provides that, deviation of these quads from initial triangles is negligibly small, but also does not allow that all triangles are merged. Thus, a mixed quadrilateral and triangular mesh is obtained. To obtain pure quadrilateral mesh each of these quadrilaterals and triangles is subdivided into four and three quadrilaterals, respectively. In this way, the initial number of quadrilaterals is greater than the initial number of triangles a bit more than two times.

The initial number of triangles can be reduced by various decimation techniques. However, as a result of decimation, some fine details of the model may be lost. To measure the geometrical discrepancy between the simplified model and the original model, we compute the Euclidian distance between each node of the original triangular mesh and its projection to the triangular or quadrilateral surface. We are interested in an average distance for all nodes, which we call the average deviation, σ_{av}, and in a maximum distance, which we call the maximum deviation, σ_{max}.

In this work, decimation is performed in such a way that the maximum deviation of initial nodes from newly created triangles is lower than the maximum allowed value σ_{max} . In addition, in a process of meshing of mixed quadrilateral and triangular mesh all new nodes are glued to the initial triangular mesh. In this way, the average deviation σ_{av} of the initial nodes from the final quadrilateral mesh is reduced when compared with deviation from the mixed mesh.

Fig. 2 shows the quadrilateral mesh for the outer surface of the phantom computed using different maximal deviations. In Fig. 3, we show the segmentation of the inner surfaces of the phantom: the boundaries of the homogeneous brain and the stroke computed for $\sigma_{max} = 3\,\mathrm{mm}$.

Tab. I gives the number of quadrilaterals and the corresponding number of unknowns (obtained for plane wave excitation), calculated for each model at the frequency $f = 1\,\mathrm{GHz}$. The range of the maximum deviation is $0.75\,\mathrm{mm} \leq \sigma_{max} \leq 4.5\,\mathrm{mm}$, and the average deviation is approximately three times less. At the same time, the number of the unknowns is $7{,}604 \leq N \leq 180{,}068$.
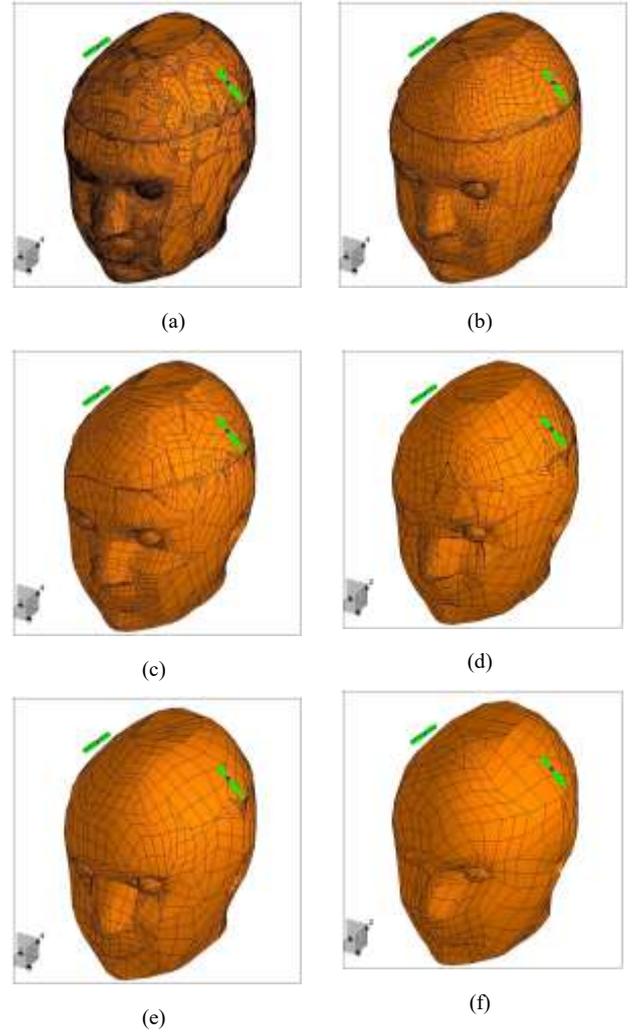

(a) (b) (c) (d) (e) (f)

Fig. 2. The outer suface of the numerical phantom represented by a quadrilateral mesh with (a) $\sigma_{max} = 0.00$ mm, (b) $\sigma_{max} = 0.75$ mm, (c) $\sigma_{max} = 1.50$ mm, (d) $\sigma_{max} = 2.25$ mm, (e) $\sigma_{max} = 3.00$ mm, and (f) $\sigma_{max} = 4.50$ mm.
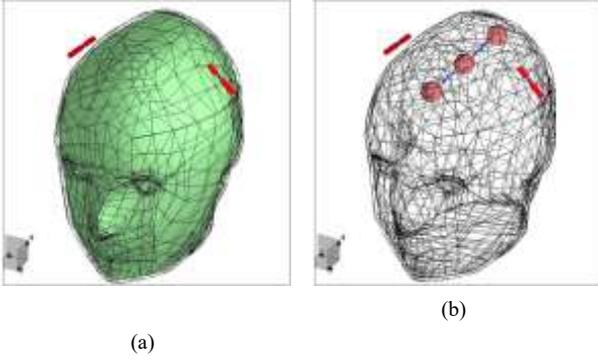
Fig. 3. The inner sufaces of the numerical phantom represented by a quadrilateral mesh (a) homogeneous brain, (b) stroke at three different locations (σ_{max} = 3 mm).

TABLE I. THE NUMBER OF UNKNOWNS FOR DIFFERENT MODELS

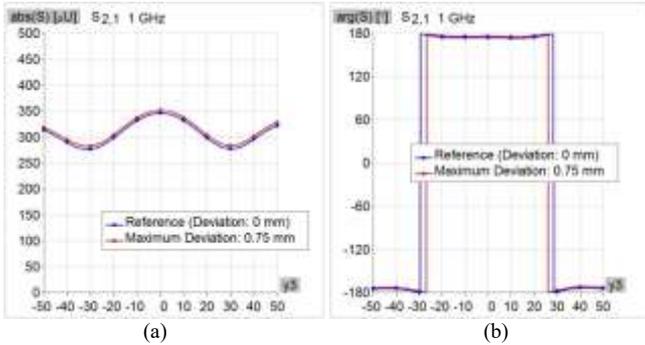| Type of mesh (STL/Quad)	Max. allowed deviation [mm]	Average deviation [mm]	Number of triangles/ quads	Number of unknowns
STL	/	/	18780	/
Quad	0.00	0.00	44797	180,068
Quad	0.75	0.26	10657	43254
Quad	1.50	0.52	5686	23226
Quad	2.25	0.78	3684	15178
Quad	3.00	0.99	2862	11774
Quad	3.75	1.25	2106	8866
Quad	4.50	1.53	1778	7604

Fig. 4. (a) Magnitude of the transmission coefficient and (b) phase of the transmission coefficient computed for the reference model and the model with σ_{max} = 0.75 mm.

To estimate the tradeoff between the reduction of the number of unknowns and the accuracy of the electromagnetic model, we studied the variation of the transmission coefficient as a function of the maximum deviation and stroke location. The stroke was located in the yz plane, and we varied its position along the y-axis for $-50\,\text{mm} \leq y \leq 50\,\text{mm}$ with 10 mm step. The central location of the stroke ($y = 0\,\text{mm}$) is a half-way between the dipoles. Fig. 3b illustrates the central and two end positions of the stroke.

First, we compared the reference model ($\sigma_{max} = 0$) and the model with the smallest deviation ($\sigma_{max} = 0.75\,\text{mm}$). Fig. 4 shows the obtained results for the magnitude and the phase of the transmission coefficient. The difference between the results was negligible: the magnitude error was around 1.4% and the phase error was around 1.4°. At the same time, the number of unknowns (including dipole antennas and stroke) was decreased from 180,170 to 43,356 unknowns. The computational times for the reference model and simplified model (for 11 stroke positions) were around 18 hours and 16 minutes, respectively. Hence, in the further analysis we used the model $\sigma_{max} = 0.75\,\text{mm}$ as the new reference model.

In the differential MWI, which is the intended application for this phantom [10], the target shape and location are found using the difference between the scattering parameters. We define the differential signal as

$$\Delta S_{12}(\sigma_{max}) = S_{12}(\sigma_{max}) - S_{12}^0(\sigma_{max}), \tag{1}$$

where the superscript 0 denotes that the transmission coefficient was computed without the stroke. To evaluate the difference between the reference model, $\sigma_{max} = 0.75\,\text{mm}$, and other more simplified models, we define the relative error

$$\varepsilon(\sigma_{max}) = \frac{\sum_{i=1}^{11}\left|\Delta S_{12}(y_i;\sigma_{max}) - \Delta S_{12}(y_i;\sigma_{max} = 0.75)\right|}{\sum_{i=1}^{11}\left|\Delta S_{12}(y_i;\sigma_{max} = 0.75)\right|}, \tag{2}$$

where the subscript i denotes the stroke position. Fig. 5 shows the magnitude and the phase of the differential signal as a function of the stroke location, for various maximum deviations. The results for $\sigma_{max} = 0.75\,\text{mm}$ and $\sigma_{max} = 1.5\,\text{mm}$ were almost the same. For higher values of maximum deviation, the difference with respect to the reference model was more pronounced. However, the discrepancy appeared mostly in the range where the differential signal was very low.
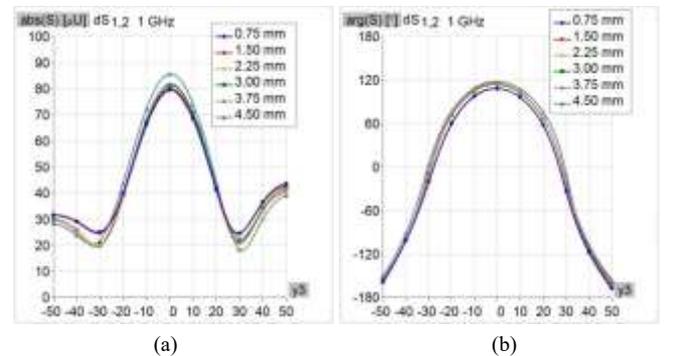

Fig. 5. (a) Magnitude and (b) phase of the differential transmission coefficient computed for various maximum deviations as a function of the stroke position.

Finally, another tool to control the number of unknowns and influence the accuracy is a reference frequency. The order of the current approximation on each quadrilateral is computed based on the reference frequency instead of true frequency. Hence, by increasing the value of the reference frequency we can improve the accuracy, yet at the cost of a larger number of unknowns. Fig. 6 shows the plots of the relative error as a function of the maximum deviation and the reference frequency. For $\sigma_{max} \leq 1.5\,\text{mm}$, the relative error was less than 5%. As expected, the relative error increases with the increase of the maximal deviation and decreases with the increase of the reference frequency. The opposite effects of the geometrical simplification and the reference frequency on the number of unknowns (together with dipole antennas and stroke) are shown in Table II.
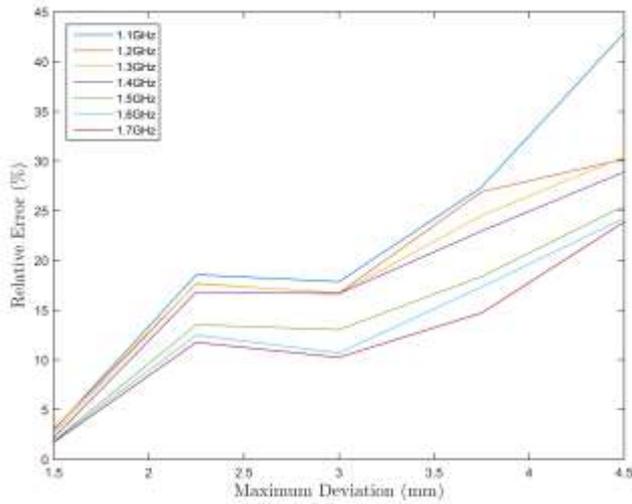

Fig. 6. Relative error as a function of the maximum deviation and the reference frequency.

TABLE II. THE NUMBER OF UNKNOWNS AS FUNCTIONS OF MAXIMAL DEVIATION AND REFERENCE FREQUENCY.

	Number of unknowns					
Max Deviation (mm)	0.75	1.50	2.25	3.00	3.75	4.50
Default Ref. Freq.	43356	23328	15280	11876	8968	7706
f_r= 1.1 GHz	43462	23410	15352	12142	9348	8186
f_r= 1.2 GHz	43588	23566	15606	12482	9742	8824
f_r= 1.3 GHz	43842	23816	15920	12894	10308	9346
f_r= 1.4 GHz	44098	24120	16494	13392	11094	9988
f_r= 1.5 GHz	44348	24454	17178	14068	11730	10994
f_r= 1.6 GHz	44702	25100	17902	15032	12840	12008
f_r= 1.7 GHz	45212	25862	18830	16240	13904	12802

IV.   CONCLUSION

In this paper we studied the simplification of the anthropomorphic phantom used for validation of the microwave imaging algorithms. Due to the very large number of triangles in the original STL model, the electromagnetic model of the phantom had an extremely large number of unknowns. By altering the model, which introduced the maximum deviation of less than 1 mm from the original model, the number of the unknowns was reduced from 180,068 to 43,254 with negligible accuracy loss. Further simplification reduced the number of the unknowns even more but affected the solution quality. In a detailed study, we showed the tradeoff between the accuracy of the electromagnetic analysis and the number of unknowns.

V.   ACKNOWLEDGMENT

REFERENCES

[1] L. Crocco, I. Karanasiou, M. James, R. Conceição, Emerging Electromagnetic Technologies for Brain Diseases Diagnostics, Monitoring and Therapy, Switzerland, Springer, 2016.

[2] R. Conceição, J. Mohr, M. O'Halloran, *An Introduction to Microwave Imaging for Breast Cancer Detection*, Switzerland, Springer, 2018.

[3] R. Scapaticci, L. D. Donato, I. Catapano, and L. Crocco, "A feasibility study on microwave imaging for brain stroke monitoring," *Progress In Electromagnetics Research B,* vol. PIERB-40, pp. 305–324, 2012.

[4] R. Scapaticci, O. M. Bucci, I. Catapano, and L. Crocco, "Differential microwave imaging for brain stroke followup," *Int. J. Antennas Propag.*, Article ID 312528, 11 pages, 2014.

[5] M. Persson et al., "Microwave-Based Stroke Diagnosis Making Global Prehospital Thrombolytic Treatment Possible*," IEEE Transactions on Biomedical Engineering,* vol. 61, no. 11, pp. 2806-2817, Nov. 2014.

[6] T. Singh, M. Stevanetic, M. Stevanovic and B. Kolundzija, "Homogenization of Voxel Models using Material Mixing Formulas," *2020 14th European Conference on Antennas and Propagation (EuCAP)*, Copenhagen, Denmark, 2020, pp. 1-4.

[7] WIPL-D Pro CAD 2019, WIPL-D d.o.o, Belgrade, 2019.

[8] Graedel, N.N.; Polimeni, J.R.; Guerin, B.; Gagoski, B.; Wald, L.L. An Anatomically Realistic Temperature Phantom for Radio Frequency Heating Measurements. Magn. Reson. Med. 2015, 73, 442–450.

[9] Joachimowicz, N.; Duchêne, B.; Conessa, C.; Meyer, O. Anthropomorphic Breast and Head Phantoms for Microwave Imaging. Diagnostics 2018, 8(4) p85 .

[10] Tobon Vasquez, J.A.; Scapaticci, R.; Turvani, G.; Bellizzi, G.; Rodriguez-Duarte, D.O.; Joachimowicz, N.; Duchêne, B.; Tedeschi, E.; Casu, M.R.; Crocco, L.; Vipiana, F. A Prototype Microwave System for 3D Brain Stroke Imaging. *Sensors* 2020, 20, 2607.

[11] B.M. Kolundzija and A.R. Djordjevic, *Electromagnetic modeling of composite metallic and dielectric structures*, Boston, London, Artech House, 2002.